Case Studies in Thermal Engineering xxx (xxxx) 103686

Contents lists available at ScienceDirect

Case Studies in Thermal Engineering

journal homepage: www.elsevier.com/locate/csite

Numerical simulation for thermal radiative flow of tangent hyperbolic nanofluid due to Riga plate in the presence of joule heating

Muhammad Jawad [a], Hassan Ali Ghazwani [b, **], Mohamed R. Ali [c, g, *], A.S. Hendy [d], Afraz Hussain Majeed [e], Xinhua Wang [f]

[a] Faculty of Sciences, The Superior University Lahore, Pakistan.
[b] Department of Mechanical Engineering, Faculty of Engineering, Jazan University, P.O Box 45124, Jazan, Kingdom of Saudi Arabia
[c] Faculty of Engineering and Technology, Future University in Egypt, New Cairo, 11835, Egypt
[d] Department of Computational Mathematics and Computer Science, Institute of Natural Sciences and Mathematics, Ural Federal University, 19 Mira St., Yekaterinburg, 620002, Russia
[e] School of Energy and Power Engineering, Jiangsu University, Zhenjiang 212013, China.
[f] College of Mechanical Engineering and Applied Electronics, Beijing University of Technology, Chaoyang District, 100124, China
[g] Basic Engineering Science Department, Benha Faculty of Engineering, Benha University, Benha, Egypt

ARTICLE INFO

Keywords:
Tangent hyperbolic fluid
Swimming microorganism
Chemical reaction
Heat source
Radiation
Mathematica

ABSTRACT

In this paper, numerical simulation for the two-dimensional flow of tangent hyperbolic fluid in the manifestation of nanoparticles, heat source and joule heating is considered. For motivation of problem, the role of Riga plate is investigated. Chemical reaction and Brownian motion are the parts of the analysis. The set of PDEs of Tangent hyperbolic nanofluids with swimming germs is converted in to couple of ODEs by employing well-known approach namely shooting scheme. The resulting highly nonlinear and coupled ODEs are solved by using ND solve tool of Wolfram Mathematica 11. Numerical outcome of involving parameters of interest like Lewis number Le, Prandtl number Pr, Chemical diffusion k, Peclet number Pe, Weissenberg number We, Bioconvection Lewis number Lb, nonlinear radiation, Biot number Bi, modified Hartmann number Q and magnetic parameter M on tangent hyperbolic nanofluids velocity f'', temperature θ, concentration φ and density of germs distribution are discussed in the form of graphical trend and tables. We professed that the speed of fluid degenerated for the increasing value of power-law index n and magnetic parameter M. The Nusselt number growths for growing values of the thermophoresis parameter Nt, Biot number Bi and radiation parameter Nr.

1. Introduction

There are numerous industrial uses for the flow of non-Newtonian fluids due to stretched sheet including polymers, food processing, textiles, etc. In modern manufacturing, non-Newtonian fluids are used more frequently than Newtonian fluids. Some additives can improve the efficacy of the fluids, increasing the range of applications. One of the variables that can be utilised to determine the desired feature's outcome and monitor the cooling rate is magneto hydrodynamics. A magnetic field and a flowing fluid (such as plasma or gas) can combine to create power in magneto hydrodynamic power plants. These tools are appropriate for producing big

* Corresponding author: Mohamed R. Ali
** Corresponding author: Hassan Ali Ghazwani
E-mail addresses: jawadsial37@gmail.com (M. Jawad), hghazwani@jazanu.edu.sa (H.A. Ghazwani), mohamed.reda@fue.edu.eg (M.R. Ali).

https://doi.org/10.1016/j.csite.2023.103686
Received 21 July 2023; Received in revised form 6 October 2023; Accepted 26 October 2023
2214-157/

amounts of power with little harm to the environment. Impressions of MHD on the stretching surface with different geometry explored by Refs. [1–4]. Model of hyperbolic tangent fluid is a preferable replacement for the conventional Newtonian model in the field of chemical engineering. This rheological model is superior to other non-Newtonian formulations because of its computational effectiveness, durability, and usefulness. The hyperbolic tangent model is kind of the non-Newtonian models that can be behaved to designate non-Newtonian fluids [5]. The Keller box technique was used by Malik et al. [6] to investigate the electrical conducting flow of hyperbolic tangent fluid underneath the influence of a stretching cylinder. Recently, Amjad et al. [7] investigated the tangent hyperbolic with magnetic field in the presence of nanoparticles due to stretched sheet. Nanofluids are widely used in a wide range of industrial systems, making them a well-liked research subject. It is employed in many different engineering and industry process to regulate temperatures and increase productivity. This popular subject has drawn the devotion of numerous academics due to its wide-ranging applications and usage. The thermal process is enhanced when nanoparticles are added to base fluids to boost thermal conductivity. The idea of nanofluids was first introduced by Choi [8], following which researchers expanded on it and investigated the unique qualities and novel characteristics of Nano fluids. The theory of heat transfer has captured the interest of numerous scientists over the past two decades owing to its extensive role in technological and manufacturing uses in a variety of disciplines, such as ordering of moisture, agricultural fields. The Riga Plate is a distinguished actuator made up of enduringly fixed magnets and electrodes that alternately produce Lorentz force that rapidly reduces as one moves away from the Riga Plate. The inspiration of Cattaneo-Christov heat on flow among Riga plates with Joule heating and absorption was studied by Ref. [9]. Rasool et al. [10] the performance of the electrical conducting fluid flows between Riga plate in the presence of heating phenomena nanoparticles. Bio-convection is a trend in which arbitrary association of micro-organisms is deliberated, it could take the shape of a single molecule or a group of molecules. Different methods of bio-convection are based on the fact that a variety of micro germs travel in the opposite direction of gravity. Some microorganisms, such as gyrotactic germs, exhibit directional motion that is counter to gravity in still water. Vincent et al. [11] demonstrate the structure of bioconvection in a suspension of swimming algae. Kada et al. [12] investigated the role of bioconvection and gyrotactic microorganism on flow of Williamson fluid in the manifestation of thermal radiation. Raizah et al. [13] explored the phenomena of gyrotactic microorganism of flow of hybrid nanofluid in the incidence of circular cylinder across stagnation point. Researchers are now studying bio-convection and interesting literature related to his work [14–38]. According to the aforementioned survey of literature, no attempt has been made to analyses theory of swimming microorganism in the magnetized flow of tangent hyperbolic Nano fluid in the presence of joule heating. In addition the role of Riga plate is consider for motivation of problem. The influence of is swimming germ is also part of this study. The governing couple of PDEs of tangent hyperbolic Nano fluid is transformed in to set of ODEs. Numerical results are achieved by using ND solve package of Mathematica. We compared the results to previously published research to validate them and found a high degree of agreement.

2. Mathematical analysis

The inclusion of solar radiation and joule heating in MHD flow of tangent hyperbolic nanofluid with heat transfer in the existence of Riga plate has been considered with the assumption as under (See Fig. 1 [39]):

- The flow is steady and two dimensional.
- The preferred coordinates are Cartesian.
- The strength of applied magnetic field in B_0 which is normal to the sheet.
- The fluid velocity is $V = V(u, v)$.
- The flow is due to stretched surface that is placed in plan y $= 0$.
- The radiative heat flux is q_r.
- The fluid is viscous and incompressible.

The governing equation of current model is defined as
Equation of mass conservation

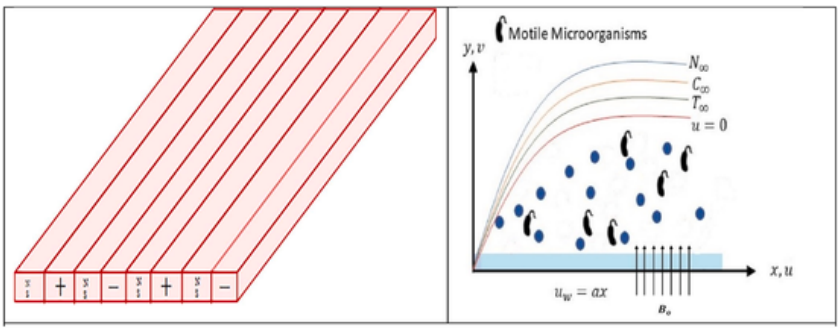

Fig. 1. Physical geometry of the problem.

$$\frac{\partial u}{\partial x}+\frac{\partial v}{\partial y}=0 \tag{1}$$

Equation of momentum

$$u\frac{\partial u}{\partial x}+v\frac{\partial v}{\partial y}=v\left(1-n\right)\frac{\partial^2 u}{\partial y^2}+\sqrt{2}vn\Gamma\left(\frac{\partial u}{\partial y}\right)\frac{\partial^2 u}{\partial y^2}+\frac{\pi J_0 M_0}{8\rho_f}\exp\left(\frac{-\pi}{b}y\right)-\frac{\sigma B_0 u}{\rho_f}, \tag{2}$$

Equation of energy

$$u\frac{\partial T}{\partial x}+v\frac{\partial T}{\partial y}=\alpha\left(\frac{\partial^2 T}{\partial y^2}\right)+\wedge\left[D_B\left(\frac{\partial C}{\partial y}\right)\left(\frac{\partial T}{\partial y}\right)+\frac{D_T}{T_\infty}\left(\frac{\partial T}{\partial y}\right)^2\right]+\frac{\sigma {B_0}^2 u^2}{\rho_f}-\frac{1}{(\rho c)_f}\frac{\partial q_r}{\partial y}, \tag{3}$$

Equation of volumetric concentration

$$u\frac{\partial C}{\partial x}+v\frac{\partial C}{\partial y}=D_B\frac{\partial^2 C}{\partial y^2}+\frac{D_T}{T_\infty}\left(\frac{\partial^2 T}{\partial y^2}\right)-K_r\left(C-C_\infty\right). \tag{4}$$

Equation of density of motile germs

$$u\frac{\partial n}{\partial x}+v\frac{\partial n}{\partial y}+\frac{bW_C}{\left(C_w-C_\infty\right)}\left[\frac{\partial}{\partial y}\left(n\frac{\partial C}{\partial y}\right)\right]=D_m\frac{\partial^2 n}{\partial y^2} \tag{5}$$

Subjected to

$$\left.\begin{array}{l} u=u_w, v=0, -K\frac{\partial T}{\partial y}=h_f\left(T_w-T\right), D_B\frac{\partial C}{\partial y}+\frac{D_T}{T_\infty}\frac{\partial T}{\partial y}=0, n=n_w \text{ at } y=0, \\ U\to U_\infty, T\to T_\infty, C\to C_\infty, n\to n_\infty \; as \; y\to\infty. \end{array}\right| \tag{6}$$

2.1. Similarity transformation

The similarity variables are illustrated as:

$$\psi=\sqrt{avxf}\left(\eta\right), \eta=\sqrt{\frac{a}{v}}y, \varphi\left(\eta\right)=\frac{C-C_\infty}{C_\infty}, \theta\left(\eta\right)=\frac{T-T_\infty}{T_w-T_\infty}, \chi\left(\eta\right)=\frac{n-n_\infty}{n_w-n_\infty}u=\frac{\partial\psi}{\partial y}, v=-\frac{\partial\psi}{\partial x}, \tag{7}$$

As a result, Eq. (1) is satisfied identically and equations (2)–(4) are transformed as:

$$\begin{aligned}&(1-n)f'''\left(\eta\right)+f\left(\eta\right)f''\left(\eta\right)+nWef'''\left(\eta\right)f''\left(\eta\right)-f'^2\left(\eta\right)-\\&Mf'\left(\eta\right)+Qexp\left(-C_1\eta\right)=0,\end{aligned} \tag{8}$$

$$\begin{aligned}&\left(1+\epsilon\theta\left(\eta\right)+\frac{4}{3}R_d\right)\theta''\left(\eta\right)+P_r f\left(\eta\right)\theta'\left(\eta\right)+P_r MEcf'^2\left(\eta\right)+\\&P_r Nb\varphi'\left(\eta\right)\theta'\left(\eta\right)+P_r Nt\theta'^2\left(\eta\right)=0,\end{aligned} \tag{9}$$

$$\varphi''\left(\eta\right)+\frac{Nt}{Nb}\theta''\left(\eta\right)+Scf\left(\eta\right)\varphi'\left(\eta\right)+Sck_1\varphi\left(\eta\right)=0, \tag{10}$$

$$\chi''\left(\eta\right)+Lbf\left(\eta\right)\chi'\left(\eta\right)-Pe\left[\varphi''\left(\eta\right)\left(\varphi\left(\eta\right)+\Omega\right)+\chi'\left(\eta\right)\varphi'\left(\eta\right)\right]=0, \tag{11}$$

The boundary conditions are transformed as:

$$\left.\begin{array}{l} f\left(0\right)=0, f'\left(0\right)=1, \theta'\left(0\right)=Bi\left(\theta\left(0\right)-1\right), Nb\varphi'\left(0\right)+Nt\theta'\left(0\right)=0, \chi\left(0\right)=1 \; at \; \eta=0, \\ f'\left(\eta\right)\to 0, \theta\left(\eta\right)\to 0, \varphi\left(\eta\right)\to 0, \chi\left(\eta\right)\to 0 \; as \; \eta\to\infty. \end{array}\right| \tag{12}$$

Where

$$\left.\begin{array}{c} \Omega=\frac{n_\infty}{n_w-n_\infty}, Pe=\frac{bW_C}{D_m}, We=\frac{\sqrt{2}a^{\frac{2}{3}}x\Gamma}{\sqrt{v}}, Rd=\frac{4\sigma^* T_\infty^3}{k^* k}. Nb=\frac{(\rho c)_p D_B(C_\infty)}{(\rho c)_f v}, \\ S_c=\frac{v}{D_B}, Lb=\frac{v}{D_m}, M=\frac{\sigma B_0^2}{\rho fa}, C_1=\frac{\pi}{b}\sqrt{\frac{v}{a}} \; \Pr=\frac{v}{\alpha}, \\ Q=\frac{\pi J_0 M_0}{8\rho_f}, Nt=\frac{(\rho c)_p D_T\left(T_f-T_\infty\right)}{(\rho c)_f v T_\infty}, Bi=\frac{h_f}{k}\sqrt{\frac{v}{a}}, \end{array}\right| \tag{13}$$

2.2. Physical quantities of interest

The physical quantities are defined as:

$$\left.\begin{array}{c} C_f = \frac{\tau_w}{\rho {u_w}^2}, Nu_x = \frac{x q_w}{k(T-T_\infty)}, \\ \tau_w = \mu\left((1-n)\frac{\partial u}{\partial y} + \frac{n\Gamma}{\sqrt{2}}\left(\frac{\partial u}{\partial x}\right)^2\right), \\ q_w = -k\left(1+\frac{16\sigma^* T_\infty^3}{3k^* k}\right)\frac{\partial T}{\partial y}. \end{array}\right| \tag{14}$$

The physical quantities in non-dimensional form:

$$\left|\begin{array}{c} C_f\sqrt{Re}_x = -\left((1-n)+\frac{n}{2}W_e f''(0)\right)f''(0), \\ Nu_x Re_x^{-1/2} = -\left(1+\frac{4}{3}N_r\right)\theta'(0), \\ Sh_x Re_x^{-1/2} = -\varphi'(0), \\ Nn_x Re_x^{-1/2} = -\chi'(0). \end{array}\right| \tag{15}$$

Where $Re_x = \frac{ax^2}{v}$ is local Reynolds number.

3. Numerical technique

The set of equations namely Eq. (7) to Eq. (9) are higher order non-linear coupled equations. It is inflexible to find any analytical solution to such a system of equations. Shooting method with built in command of Wolfram Mathematica 11 is well known approach to find numerical solution of such type of problem. Shooting steps are given below

$$\left.\begin{array}{c} f''' = \frac{1}{(1-n)+nW_e f''}\left[f'^2 + Mf' - ff'' - Qexp\left(-C_1\eta\right)\right], \\ \theta'' = -\frac{\Pr}{\left(1+\epsilon\theta+\frac{4}{3}N_r\right)}\left[f\theta' + Nb\varphi'\theta' + Nt\theta'^2 + MEcf'^2\right], \\ \varphi'' = \frac{Nt}{Nb}\theta'' - fSc\varphi' - Sck_1\varphi, \\ \chi'' = Pe\left[\varphi''(\varphi+\Omega) + \chi'\varphi'\right] - Lbf\chi'. \end{array}\right| \tag{15}$$

Boundary condition in dimensionless shape is:

$$\left|\begin{array}{c} y_1(\eta) = 0, y_2(\eta) = 1, y_5(\eta) = Bi(y_4(\eta) - 1), \\ Nby_7(\eta) + Nty_5(\eta) = 0 \; y_8(\eta) = 0, as \quad \eta = 0, \\ y_2(\infty) \to 0, y_4(\infty) \to 0, y_6(\infty) \to 0, y_8(\infty) \to 0 \quad as \quad \eta \to \infty \end{array}\right| \tag{16}$$

Let us put $f = f_1, f' = f_2, f'' = f_3, f''' = f_3', \theta = f_4, \theta' = f, \theta'' = f_5', \varphi = f_6, \varphi' = f_7, \varphi'' = f_7', \chi'' = f_8'$. equations (15) and (16) are written as:

$$\left.\begin{array}{c} f_1' = f_2 \\ f_2' = f_3 \\ f_3' = \frac{f_2^2 + Mf_2 - f_1 f_3 - Qexp(-C_1\eta)}{(1-n)+nWef_3} \\ y_4' = y_5 \\ f_5' = \frac{-\Pr\left(f_1 f_5 + Nbf_7 f_5 + Ntf_5^2 + 2MEcf_2^2\right)}{\left(1+\epsilon f_4+\frac{4}{3}Nr\right)} \\ f_6' = f_7 \\ f_7' = -Scf_1 f_7 - Sckf_7 + \frac{Nt}{Nb}f_5' \\ y_8' = y_9 \\ f_9' = Pe\left[f_7'\left(f_8+\Omega\right)f_7 f_9\right] - Lbf_1 f_9 \end{array}\right| \tag{17}$$

$$\left.\begin{array}{c} f_1(0) = 0, f_2(0) = 1, f_3(0) = l \quad f_4(0) = m \\ f_5(0) = Bi(t-1), f_6(0) = n \quad f_7(0) = -\frac{Nt}{Nb}Bi(t-1) \end{array}\right| \tag{18}$$

4. Results and discussion

In current section, a detailed computational effort is made to observe the influence of emerging parameters like Lewis number Le, Prandtl number Pr, Peclet number Pe, Weissenberg number We, Bioconvection Lewis number Lb, nonlinear radiation, Biot number Bi, modified Hartmann number Q and magnetic parameter M. The physical quantities namely non-dimensional tangent hyperbolic nanofluids velocity f'', temperature θ, concentration φ and density of germs distribution χ have been mapped for representative values of the above mentioned parameters to reveal the physical behavior of the problem. The effect of parameter M on $f(\eta)$ is offered in

Fig. (2) The flow speed is reduced with increase in values of M. It is because with the increase in magnetic field strength, the value of opposing force namely Loretnz force is increased. The consequence of parameter M on $\theta(\eta)$ is existing in Fig. (3). Temperature distribution $\theta(\eta)$ enhances with increase in values of M, the magnetic parameter because the resulting Lorentz force causes a resistance to flow and hence increases the temperature of fluid. The inspiration of the parameter n for velocity field $f'(\eta)$ is dispatched in Fig. (4). The flow speed is diminished with escalation in values of power-law index n. Physically, more resistance is delivered to fluid speed by growing the magnitude of n as result the speed of fluid is declined due to the shear thinning. The significance of Pr on $\theta(\eta)$ is indicated in Fig. (5). It is detected that for growing value of the Pr fluid temperature falls, this is because increasing values of Prandtl number result in a decrease in the rate of heat transfer. The proportion of momentum to thermal diffusivity is known as the Prandtl number. Pr regulates the relative thickening of the momentum and thermal boundary layers in heat transfer problems. Fig. (6) illustrates the ef-

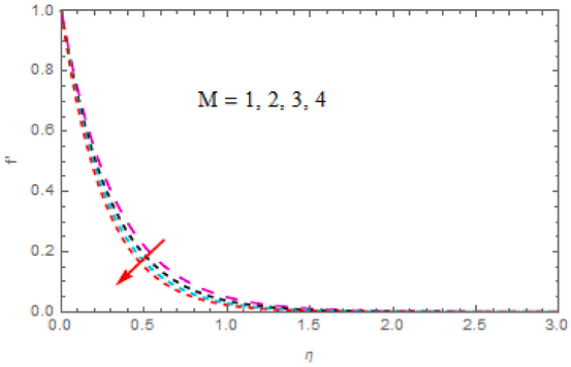

Fig. 2. Plot for $f'(\eta)$ under the influence of M.

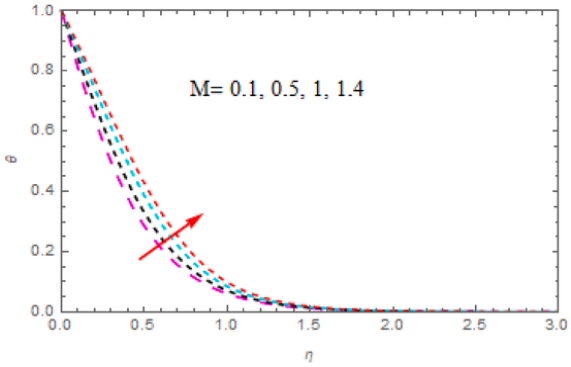

Fig. 3. Plot for $\theta(\eta)$ under the influence of M.

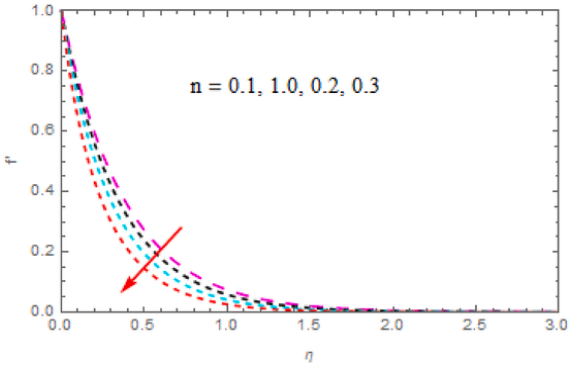

Fig. 4. Plot for $f'(\eta)$ under the influence of n.

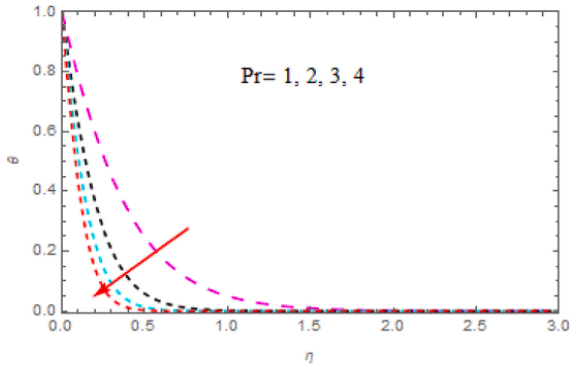

Fig. 5. Plot for $\theta(\eta)$ under the influence of Pr .

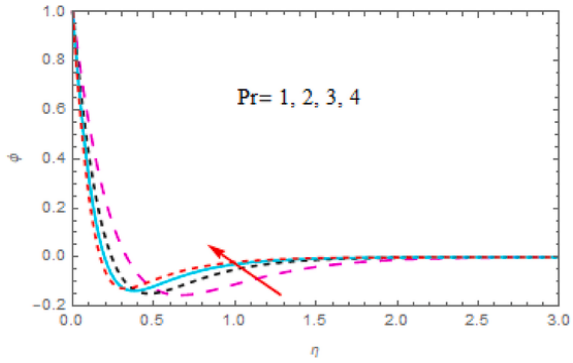

Fig. 6. Plot for $\varphi(\eta)$ under the influence of Pr .

fect of the Pr on the volumetric concentration function $\varphi(\eta)$. It suggests that an upsurge in Pr causes a decline in the mass friction layer $\varphi(\eta)$. The implication of Small Quantity parameter ϵ on $\theta(\eta)$ is designated in Fig. (7). This occurs because as ϵ increases, the kinetic energy increases and leads to an enlarge in temperature. The action of thermal radiation on the temperature field is depicted in Fig. (8). The rising temperature of fluid can be seen as one of the main indicators of thermal radiation Rd. Additionally, the boundary layer's thickness has grown. The act of thermophoresis parameter Nt on the temperature function $\theta(\eta)$ are portrayed in Fig. (9). It is noted that temperature distribution display an rise for mounting values of thermophoresis parameter Nt. Substantially, hot particles move away from surface of highly temperatures faster than cold particles, causing the temperature of the fluid to rise. The performance of parameter Nb on the temperature function $\theta(\eta)$ are described in Fig. (10). Brownian motion come from the combination of nanoparticles and fluid. It has been demonstrated that increasing the Brownian motion volumetric concentration increases the phenomena of random collision among the nanoparticles present in the base fluid (liquid and gas), resulting in a decrease in the mass

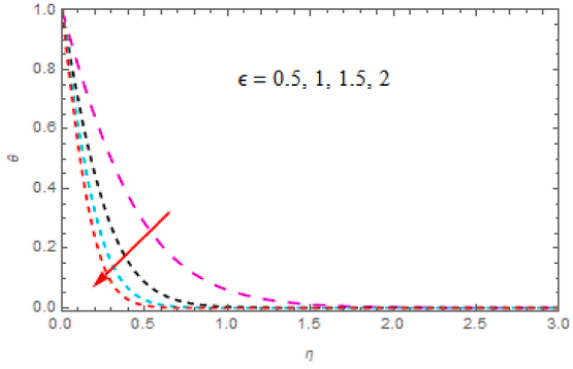

Fig. 7. Plot for $\theta(\eta)$ under the influence of ϵ.

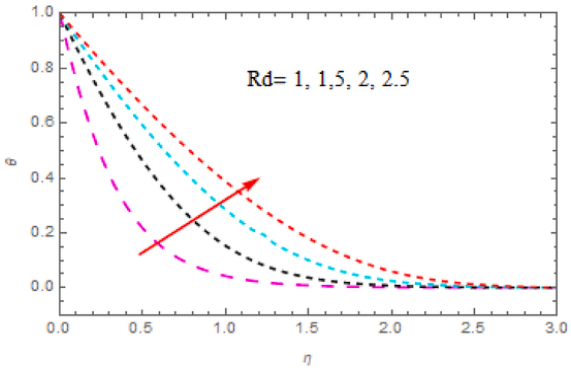

Fig. 8. Plot for $\theta(\eta)$ under the influence of Rd.

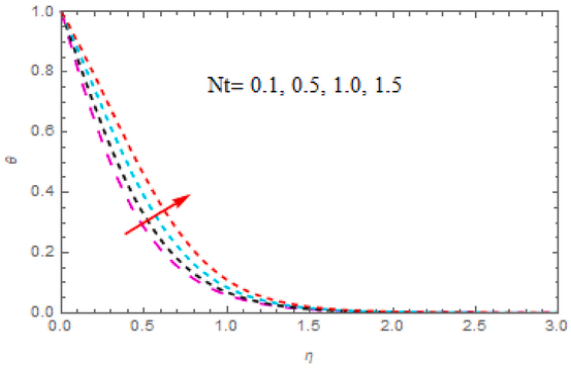

Fig. 9. Plot for $\theta(\eta)$ under the influence of Nt.

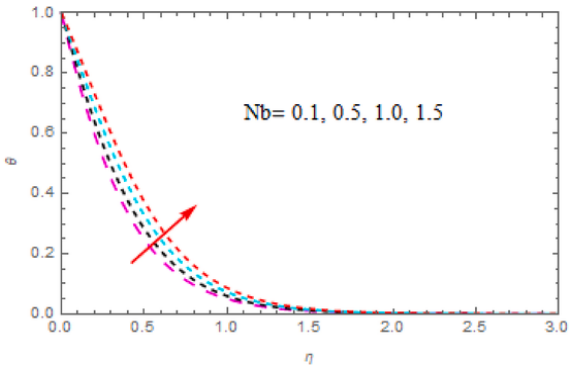

Fig. 10. Plot for $\theta(\eta)$ under the influence of Nb.

fraction field. The significance of parameter Schmidt number Sc on $\varphi(\eta)$ is signposted in Fig. (11). It is detected that for growing value of the Schmidt number Sc fluid concentration profile falls. While the thickness of the thermal boundary layer reduces as the Schmidt number rises, concentration does. Thus, as Schmidt number rises. The effect of the micro germs concentration difference Ω on the density of swimming germs $\chi(\eta)$ is shown in Fig (12). An rise in Ω leads to a reduction in $\chi(\eta)$ as the concentration of microorganisms in ambient fluid declines. The effect of the bioconvection Lewis parameter Lb on the density of motile germs is shown in Fig (13). An increase in Lb causes an increase in the density of motile germs by reducing the diffusivity of microbes. The impression of Peclet number Pe on the density field is seen in Fig. (14). Species move from surface of high concentration to those with lower concentrations during the diffusion process. It is discovered that as Pe is increased, microorganism diffusivity decreases. The ratio of advection and diffusion brought on by heat transfer is represented by the Peclet number, often spelt Péclet number. The effects of convection on thermal transport increase with increasing Péclet number. The density of motile microorganisms decreases as a result. Table 1 pre-

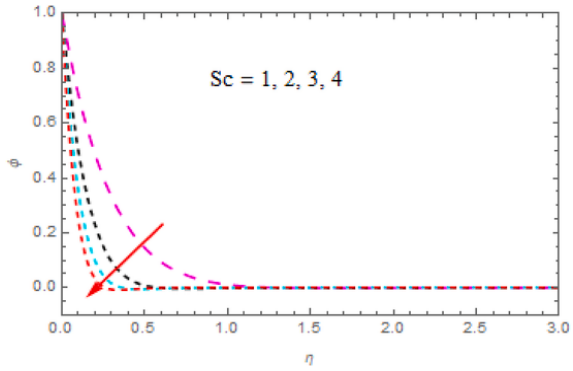

Fig. 11. Plot for $\varphi(\eta)$ under the influence of Sc.

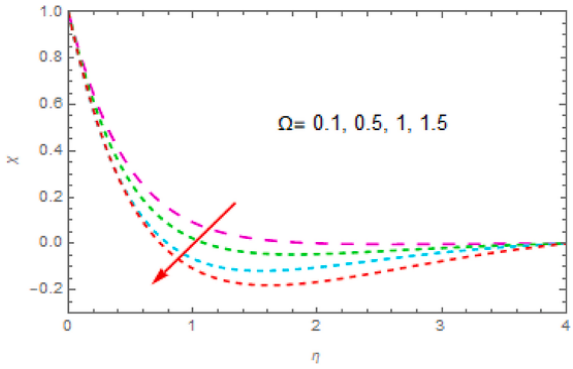

Fig. 12. Plot for $\chi(\eta)$ under the influence of Ω.

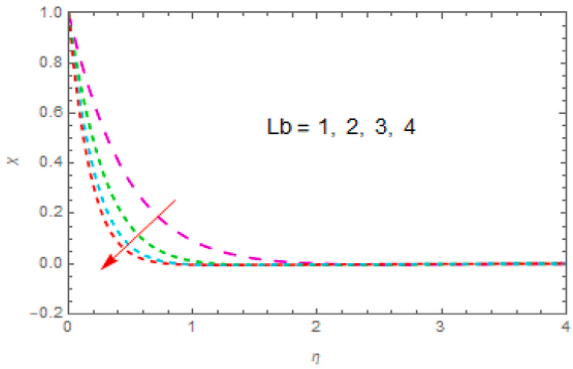

Fig. 13. Plot for $\chi(\eta)$ under the influence of Lb.

sents a good comparison of the present results for $f''(0)$ with previous results. Numerical computation of $f''(0)$ using ND-Solve command for different values of M, We and n portrayed in Table 2. Computational results of $\theta'(0)$ for different values of Q, M, Nt, We, Bi, Δ, Pr, Nb and n.are shown in Table 3. Computational outcomes of $-\varphi'(0)$ for different values of M, We, Sc and Pr described in Table 4. Impact of different values of M, Lb and Pe on $-\chi'(0)$ premeditated in Table 5.

5. Conclusion

This research has been devised to examine the impressions of chemical reaction, joule heating and thermal radiations on magneto-hydrodynamic flow of tangent hyperbolic nanofluid in the manifestation of thermopherosis encouraged by a Riga plate. Non-Newtonian fluids, commonly referred to as hyperbolic fluids, exhibit characteristics that are different from those of Newtonian fluids

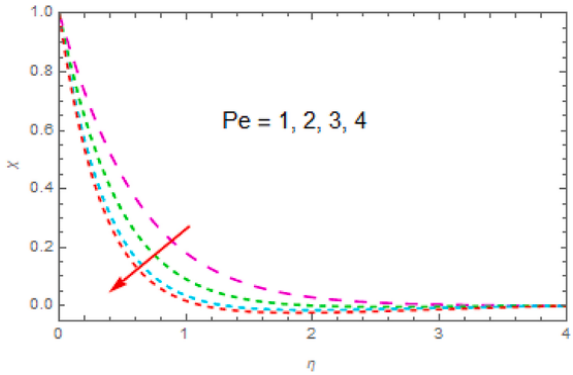

Fig. 14. Plot for $\chi(\eta)$ under the influence of Pe.

Table 1
Comparison of $f''(0)$ for different values of M when $n = 0$ and $We = 0$ with published literature.

$f''(0)$				
M	Amjad et al. [3]	Khan et al. [2]	Malik et al. [1]	Present
0.0	−1.0000	−1.0	−1.0	−1.0000
0.5	−1.11802	−1.1180	−1.11802	−1.11803
1.0	−1.41421	−1.4139	−1.41419	−1.41419
5.0	−2.449489	−2.4499	−2.44945	−2.44946

Table 2
Numerical outcomes of $f''(0)$ for different values of M, We and n.

We	n	M	$-\left((1-n)+\frac{n}{2}W_e f''(0)\right)f''(0)$
0.1	0.2	0.2	1.034661
0.2			1.020855
0.4			1.006350
	0.1		1.189353
	0.2		1.102479
	0.3		1.006255
		0.2	0.977480
		0.3	1.006257
		0.4	1.034306

like water or air. When exposed to stress or shear, they display unusual behaviour. Practical application of such kind of fluid are in food industry, cosmetics, pharmaceuticals, paints and coatings, biomedical engineering, Polymer Processing.

The main findings are listed below:

- An increase in the values of the power-law index n and magnetic parameter M, momentum boundary layer is diminished while temperature distribution is improved.
- For enhancing values of Prandtl number Pr, temperature boundary layer boosts.
- The Nusselt number growths for growing values of the Biot number Bi, radiation parameter Nr and thermophoresis parameter Nt.
- It is described that for improving values of the Schmidt number Sc, Weissenberg number We, mass friction layer reduced.
- Enhancing values of the Weissenberg number We, speed of fluids boosts.
- An escalation in the values of the bioconvection Lewis parameter Lb, concentration difference Ω and Peclet number Pe, density of swimmings is diminished.

Author contributions

Conceptualization and software MJ; Methodology, Revision, HAG, MRA and ASH; Supervision, XW; Final draft AHM, MRA and ASH. All the authors equally contributed. All authors reviewed the manuscript.

Acknowledgment: The authors extend their appreciation to the Deputyship for Research & Innovation, Ministry of Education in Saudi Arabia for funding this research work through the project number ISP23-66

Table 3
Results of $\theta'(0)$ for different values of Q, M, Nt, We, Bi, Δ, Pr, Nb and n.

We	Δ	M	Pr	Nt	Nb	Bi	n	Q	$-\left(1+\frac{4}{3}N_r\right)\theta'(0)$
1.0	0.2	0.2	2.0	0.3	0.3	2.1	0.3	0.3	0.55596
1.5									0.55054
2.0									0.54165
	0.1								0.57745
	0.5								0.65393
	0.8								0.71298
		0.1							0.44795
		0.5							0.44258
		0.8							0.44445
			1						0.89645
			2.5						1.10443
			5						1.23565
				0.1					0.56826
				0.4					0.55267
				0.7					0.53727
					0.1				0.55725
					0.4				0.55818
					0.7				0.55827
						1.1			0.47186
						1.5			0.52225
						2.0			0.57202
							0.1		0.457058
							0.2		0.437514
							0.3		0.403745
								0.1	0.577313
								0.5	0.653850
								0.8	0.712879

Table 4
Numerical outcomes of $-\varphi'(0)$ for different values of M, We, Sc and Pr.

We	M	Pr	Sc	$-\varphi'(0)$
1.0	0.2	2.0	0.3	0.0678125
2.0				0.0528934
3.0				0.0519273
	0.1			0.0720403
	0.2			0.0678123
	0.3			0.0646545
		1		0.2726637
		2.5		0.215299
		5		0.1622426
			1.0	0.0678125
			4.0	0.4200238
			5.0	0.6103582

Table 5
Numerical outcomes of $-\chi'(0)$ for different values of M, Lb and Pe.

Pe	Lb	M	$-\chi(0)$
0.1	0.4	0.3	1.0419246
0.4			1.4117438
0.8			1.7893844
	1.1		0.7017543
	1.5		0.8332579
	2.0		1.0054532
		0.1	0.4524297
		0.5	0.3436362
		1.0	0.2607936

Declaration of competing interest

The authors declare that they have no known competing financial interests or personal relationships that could have appeared to influence the work reported in this paper.

Data availability

Data will be made available on request.

Nomenclature

Viscosity μ
Stress tensor τ
Kinematic viscosity υ
Thermal conductivity κ
Wall shear stress τ_w
Thermal diffusivity α
Dimensionless similarity variable η
Thermal conductivity parameter ϵ
Prandtl number Pr
Weissenberg number We
Eckert number Ec
Free stream velocity U_∞
Specific heat Cp
Wall temperature T_∞
Skin friction coefficient C_f
Brownian motion parameter Nb
Cell swimming speed W_C
Bioconvection Lewis number Lb

References

[1] N.S. Akbar, A. Ebai, Z.H. Khan, Numerical analysis of magnetic field effects on Eyring–Powell fluid flow towards a stretching sheet, J. Magn. Magn Mater. 382 (2015) 355–358.
[2] F. Mabood, W.A. Khan, A.I.M. Ismail, MHD boundary layer flow and heat transfer of nanofluids over a nonlinear stretching sheet: a numerical study, J. Magn. Magn Mater. 374 (2015) 569–576.
[3] S. Nadeem, R. Mehmood, N.S. Akbar, Combined effects of magnetic field and partial slip on obliquely striking rheological fluid over a stretching surface, J. Magn. Magn Mater. 378 (2015) 457–462.
[4] A.K. Abdul Hakeem, N.V. Ganesh, B. Ganga, Magnetic field effect on second order slip flow of nanofluid over a stretching/shrinking sheet with thermal radiation effect, J. Magn. Magn Mater. 381 (2015) 243–257.
[5] I. Pop, D.B. Ingham, Convective Heat Transfer: Mathematical and Computational Modelling of Viscous Fluids and Porous Media, Elsevier, 2001.
[6] M.Y. Malik, T. Salahuddin, A. Hussain, S. Bilal, MHD flow of tangent hyperbolic fluid over a stretching cylinder: using Keller box method, J. Magn. Magn Mater. 395 (2015) 271–276.
[7] M. Amjad, M.N. Khan, K. Ahmed, I. Ahmed, T. Akbar, S.M. Eldin, Magnetohydrodynamics tangent hyperbolic nanofluid flow over an exponentially stretching sheet: numerical investigation, Case Stud. Therm. Eng. 45 (2023) 102900.
[8] S.U. Choi, J.A. Eastman, Enhancing the Thermal Conductivity of Fluids with Nanoparticles (No. ANL/MSD/CP-84938; CONF-951135-29), Argonne National Lab., IL (United States), 1995.
[9] M.D. Shamshuddin, P.S. Narayana, The combined effect of viscous dissipation and Joule heating on MHD flow past a Riga platewithCattaneo-Christovheatflux, Indian J. Phys. (2019) 1–10.
[10] G. Rasool, T. Zhang, A. Shafiq, Second-grade nano-fluidic flow past a convectively heated vertical Riga plate, Phys. Scripta 94 (12) (2019) 125212.
[11] R.V. Vincent, N.A. Hill, Bioconvection in a suspension of phototacticalgae, J. Fluid Mech. 327 (1996) 343–371.
[12] B. Kada, I. Hussain, A.A. Pasha, W.A. Khan, M. Tabrez, K.A. Juhany, R. Othman, Significance of gyrotactic microorganism and bioconvection analysis for radiative Williamson fluid flow with ferromagnetic nanoparticles, Therm. Sci. Eng. Prog. 39 (2023) 101732.
[13] Z. Raizah, A. Saeed, M. Bilal, A.M. Galal, E. Bonyah, Parametric simulation of stagnation point flow of motile microorganism hybrid nanofluid across a circular cylinder with sinusoidal radius, Open Phys. 21 (1) (2023) 20220205.
[14] R. Safdar, I. Gulzar, M. Jawad, W. Jamshed, F. Shahzad, M.R. Eid, Buoyancy force and Arrhenius energy impacts on Buongiorno electromagnetic nanofluid flow containing gyrotactic microorganism, Proc. IME C J. Mech. Eng. Sci. 236 (17) (2022) 9459–9471.
[15] M. Jawad, F. Mebarek-Oudina, H. Vaidya, P. Prashar, Influence of bioconvection and thermal radiation on MHD Williamson nano Casson fluid flow with the swimming of gyrotactic microorganisms due to porous stretching sheet, Journal of Nanofluids 11 (4) (2022) 500–509.
[16] R. Safdar, M. Jawad, S. Hussain, M. Imran, A. Akgül, W. Jamshed, Thermal radiative mixed convection flow of MHD Maxwell nanofluid: implementation of Buongiorno's model, Chin. J. Phys. 77 (2022) 1465–1478.
[17] M. Jawad, K. Shehzad, R. Safdar, Novel computational study on MHD flow of nanofluid flow with gyrotactic microorganism due to porous stretching sheet, Punjab Univ. J. Math. 52 (12) (2021).
[18] M. Jawad, M.K. Hameed, A. Majeed, K.S. Nisar, Arrhenius energy and heat transport activates effect on gyrotactic microorganism flowing in Maxwell bio-nanofluid with Nield boundary conditions, Case Stud. Therm. Eng. 41 (2023) 102574.
[19] M. Jawad, Insinuation of arrhenius energy and solar radiation on electrical conducting Williamson nano fluids flow with swimming microorganism: completion of buongiorno's model, East European Journal of Physics (1) (2023) 135–145.
[20] M. Jawad, M. Muti-Ur-Rehman, K.S. Nisar, Bioconvection effects on non-Newtonian chemically reacting Williamson nanofluid flow due to stretched sheet with heat and mass transfer, East European Journal of Physics (2) (2023) 359–369.
[21] P.S. Reddy, P. Sreedevi, Effect of Cattaneo–Christov heat flux on heat and mass transfer characteristics of Maxwell hybrid nanofluid flow over stretching/shrinking sheet, Phys. Scripta 96 (12) (2021) 125237.
[22] P. Sreedevi, P.S. Reddy, A.J. Chamkha, Heat and mass transfer analysis of nanofluid over linear and non-linear stretching surfaces with thermal radiation and chemical reaction, Powder Technol. 315 (2017) 194–204.

[23] P. Sreedevi, P.S. Reddy, Effect of SWCNTs and MWCNTs Maxwell MHD nanofluid flow between two stretchable rotating disks under convective boundary conditions, Heat Tran. Asian Res. 48 (8) (2019) 4105–4132.
[24] P. Sreedevi, P.S. Reddy, A.J. Chamkha, Magneto-hydrodynamics heat and mass transfer analysis of single and multi-wall carbon nanotubes over vertical cone with convective boundary condition, Int. J. Mech. Sci. 135 (2018) 646–655.
[25] P. Sreedevi, P.S. Reddy, A.J. Chamkha, Heat and mass transfer analysis of nanofluid over linear and non-linear stretching surfaces with thermal radiation and chemical reaction, Powder Technol. 315 (2017) 194–204.
[26] P. Sreedevi, P.S. Reddy, Combined influence of Brownian motion and thermophoresis on Maxwell three-dimensional nanofluid flow over stretching sheet with chemical reaction and thermal radiation, J. Porous Media 23 (4) (2020).
[27] P. Sreedevi, P.S. Reddy, Williamson hybrid nanofluid flow over swirling cylinder with Cattaneo–Christov heat flux and gyrotactic microorganism, Waves Random Complex Media (2021) 1–28.
[28] P.S. Reddy, P. Sreedevi, A.J. Chamkha, Heat and mass transfer flow of a nanofluid over an inclined plate under enhanced boundary conditions with magnetic field and thermal radiation, Heat Tran. Asian Res. 46 (7) (2017) 815–839.
[29] P.S. Reddy, P. Sreedevi, Effect of thermal radiation and volume fraction on carbon nanotubes based nanofluid flow inside a square chamber, Alex. Eng. J. 60 (1) (2021) 1807–1817.
[30] P. Sudarsana Reddy, P. Sreedevi, Impact of chemical reaction and double stratification on heat and mass transfer characteristics of nanofluid flow over porous stretching sheet with thermal radiation, Int. J. Ambient Energy 43 (1) (2022) 1626–1636.
[31] K.G. Kumar, Exploration of flow and heat transfer of non-Newtonian nanofluid over a stretching sheet by considering slip factor, Int. J. Numer. Methods Heat Fluid Flow 30 (4) (2020) 1991–2001.
[32] M.G. Reddy, M.S. Rani, M.M. Praveen, K.G. Kumar, Comparative study of different non-Newtonian fluid over an elaborated sheet in the view of dual stratified flow and ohmic heat, Chem. Phys. Lett. 784 (2021) 139096.
[33] K. Ganesh Kumar, Scrutinization of 3D flow and nonlinear radiative heat transfer of non-Newtonian nanoparticles over an exponentially sheet, Int. J. Numer. Methods Heat Fluid Flow 30 (4) (2019) 2051–2062.
[34] G.R. Machireddy, M.M. Praveena, N.G. Rudraswamy, G.K. Kumar, Impact of Cattaneo–Christov heat flux on hydromagnetic flow of non-Newtonian fluids filled with Darcy–Forchheimer porous medium, Waves Random Complex Media (2021) 1–18.
[35] M.G. Reddy, M.R. Krishnamurthy, M.M. Praveena, L.S. Naik, D.G. Prakasha, K. Ganesh Kumar, Unsteady Absorption Flow and Dissipation Heat Transfer over a Non-newtonian Fluid, Waves in Random and Complex Media, 2022, pp. 1–15.
[36] L.S. Naik, D.G. Prakasha, M.M. Praveena, M.R. Krishnamurthy, K. Ganesh Kumar, Stratification flow and variable heat transfer over different non-Newtonian fluids under the consideration of magnetic dipole, Int. J. Mod. Phys. B (2023) 2450071.
[37] K.G. Kumar, S. Manjunatha, B.J. Gireesha, F.M. Abbasi, S.A. Shehzad, Numerical illustrations of 3D tangent hyperbolic liquid flow past a bidirectional moving sheet with convective heat transfer at the boundary, Heat Tran. Asian Res. 48 (5) (2019) 1899–1912.
[38] K.G. Kumar, B.J. Gireesha, M.R. Krishanamurthy, N.G. Rudraswamy, An unsteady squeezed flow of a tangent hyperbolic fluid over a sensor surface in the presence of variable thermal conductivity, Results Phys. 7 (2017) 3031–3036.
[39] Z. Iqbal, E. Azhar, Z. Mehmood, E.N. Maraj, Melting heat transport of nanofluidic problem over a Riga plate with erratic thickness: use of Keller Box scheme, Results Phys. 7 (2017) 3648–3658.